LPV Model Order Reduction by Parameter-Varying Oblique Projection

Julian Theis, Peter Seiler, and Herbert Werner

***Abstract*—A method to reduce the dynamic order of linear parameter-varying (LPV) systems in grid representation is developed in this paper. It consists of an oblique projection and is novel in its use of a parameter-varying kernel to define the direction of this projection. Parameter-varying state transformations in general lead to parameter rate dependence in the model. The proposed projection avoids this dependence and maintains a consistent state space basis for the reduced-order system. This extension of the projection framework lends itself very naturally to balanced truncation and related approaches that employ Gramian-based information to quantify the importance of subspaces. The proposed method is used in this paper to approximate balancing and truncation for two LPV systems: the longitudinal dynamics model of an aeroservoelastic unmanned aerial vehicle and the far wake model of a wind farm.**

***Index Terms*—Linear parameter-varying (LPV) systems, model order reduction**

I. Introduction

A METHOD to reduce the number of states of linear parameter-varying (LPV) systems in grid representation is developed in this paper. LPV models are particularly useful for the design and analysis of gain-scheduled controllers due to the availability of powerful synthesis techniques and computational tools [1], [2]. Both analysis and synthesis require the solution of linear matrix inequalities (LMIs). The required computation for this solution grows rapidly with increasing state dimension and hence limits applicability to models with relatively few states. With current tools, models with an order of about 50 states are tractable. For many physically motivated models, directly obtaining models with such a low number of states is not easy. For instance, structural mechanics models are often obtained from finite element analysis with a dense grid of nodes and hence these models have a large number of states. Similarly, unsteady aerodynamic models often have several thousands of states. The method proposed in this paper can be used to obtain low-order models that can be used for LPV analysis and synthesis. It thus helps to increase the applicability of LPV control techniques to models that are otherwise out of the scope.

LPV model order reduction was first addressed in [3], [4] by generalizing the concept of balancing and truncation [5]. Balancing and truncation consists of a state space coordinate transformation followed by removing states that are considered negligible in the new coordinates. The procedure requires the solution of LMIs to obtain generalized Gramians. Hence, this approach suffers from the same computational limitations as LPV analysis and synthesis problems. In addition, LPV balancing in general involves parameter-varying transformations. Parameter-varying transformations acknowledge the parameter-dependence of the dynamic system but introduce additional rate terms. In order to avoid this rate dependence, possibly conservative constant transformations have to be used. Model order reduction by parameter-varying oblique projection takes a middle ground and allows part of the transformation to be parameter-varying while another part is kept constant. It turns out that these two parts have clear interpretations in terms of test and basis spaces in the Petrov-Galerkin approximation of dynamic systems. The main technical contribution is thus a possibility to use a partially parameter-varying transformation without the introduction of additional rate dependence. This extension of the projection framework relates very naturally to balanced truncation and related approaches that employ Gramian-based information to quantify the importance of subspaces for model order reduction. By considering linear time invariant (LTI) Gramians at fixed parameter values, it becomes possible to approximate balancing and truncation for LPV systems without the need to solve LMIs.

Several other approaches have been proposed for LPV model order reduction that use LTI techniques for frozen-parameter models and then seek to interpolate the reduced-order models for time-varying parameters, e. g., [6]–[10]. These approaches in general struggle with maintaining a consistent state space base basis for the reduced-order system. This problem is avoided by using the parameter-varying oblique projection proposed in this paper. In recent years, the problem of *parametric model reduction* has also received considerable attention, e. g., [11]–[13]. Parametric model reduction considers only constant parameter values and the goal is to approximate a family of parameterized LTI models. This differs substantially from the *LPV model order reduction* problem studied in this paper which considers time-varying parameter values and whose goal is to approximate an LPV model. The proposed method nevertheless includes parametric models as a special case of LPV systems, and can hence also be applied to this problem class.

The present paper describes parameter-varying projection as a versatile order reduction method for LPV systems. It extends the results of [14] and demonstrates the effectiveness of the approach on two detailed application examples. The first example is the high-fidelity model of the longitudinal

J. Theis and P. Seiler are with the Department of Aerospace Engineering and Mechanics, University of Minnesota, Minneapolis, MN, 55414 USA e-mail: {theis476,seile017}@umn.edu. Address all correspondence to J. Theis.
This work was supported by NASA NRA No. NNX14AL36A entitled *"Lightweight Adaptive Aeroelastic Wing for Enhanced Performance Across the Flight Envelope."* John Bosworth is the technical monitor.
H. Werner is with the Institute of Control Systems, Hamburg University of Technology, 21073 Hamburg, Germany e-mail: h.werner@tuhh.de.
Manuscript received XXX XXX; revised XXX, XXX.

dynamics of a small unmanned aeroservoelastic aircraft, where the number of states is reduced from 48 to 12. The second example is a model for unsteady aerodynamics in a wind farm, where a reduction from 20502 to 6 states is achieved.

II. Background

LPV systems are dynamic systems whose state space matrices are continuous functions of a time-varying parameter vector $\rho(t) \in \mathbb{R}^{n_\rho}$. Based on physical considerations, the admissible parameter trajectories are confined to a compact set $\mathcal{P} \subset \mathbb{R}^{n_\rho}$. This infinite dimensional set is commonly approximated by a finite dimensional subset $\{\rho_k\}_{k=1}^{n_g} \subset \mathcal{P}$, called a grid. The state space equations for an LPV system with state vector $x(t) \in \mathbb{R}^{n_x}$, input vector $u(t) \in \mathbb{R}^{n_u}$, and output vector $y(t) \in \mathbb{R}^{n_y}$ are

$$\begin{aligned} \dot{x}(t) &= A(\rho(t))\, x(t) + B(\rho(t))\, u(t) \\ y(t) &= C(\rho(t))\, x(t) + D(\rho(t))\, u(t). \end{aligned} \tag{1}$$

The problem of LPV model order reduction consists of finding an approximation for the dynamic system (1) as

$$\begin{aligned} \dot{z}(t) &= A_{\text{red}}(\rho(t))\, z(t) + B_{\text{red}}(\rho(t))\, u(t) \\ y(t) &= C_{\text{red}}(\rho(t))\, z(t) + D_{\text{red}}(\rho(t))\, u(t)\ . \end{aligned} \tag{2}$$

The reduced state $z(t) \in \mathbb{R}^{n_z}$ should be of much lower dimension than $x(t) \in \mathbb{R}^{n_x}$, while the input-output behavior from u to y should be as similar as possible to that of the original model. Further, stability of the original model should be preserved in the reduced-order model.

In the remainder of this paper, time dependence is dropped and parameter dependence is denoted by the subscript ρ, i. e., $A_\rho := A(\rho(t))$.

A. Balancing and Truncation

In order to simplify the presentation of the background material, a fixed parameter $\rho = \rho_k$ is considered. Thus, system (1) simplifies to the standard LTI system

$$\begin{aligned} \dot{x} &= A\, x + B\, u \\ y &= C\, x + D\, u\ . \end{aligned} \tag{3}$$

A standard model reduction method for LTI systems is *balancing and truncation* [5]. It requires the controllability Gramian X_c and the observability Gramian X_o that are obtained as solutions to the Lyapunov equations

$$A\, X_\text{c} + X_\text{c} A^T + B\, B^T = 0\ , \tag{4a}$$

$$A^T X_\text{o} + X_\text{o}\, A + C^T C = 0\ . \tag{4b}$$

Given a state x_0, the minimum energy required to steer the system from $x = 0$ to $x = x_0$ is $\epsilon_\text{c} = x_0^T X_\text{c}^{-1} x_0$. Further, $\epsilon_\text{o} = x_0^T X_\text{o}\, x_0$ is the energy of the free response to the initial condition x_0 [5]. The ratio $\epsilon_\text{o}/\epsilon_\text{c}$ thus measures how much a state is affected by the input and how much it affects the output. A balancing transformation $\left[\begin{smallmatrix} x_1 \\ x_2 \end{smallmatrix}\right] = T x$ can be calculated so that $T\, X_\text{c}\, T^T = (T^{-1})^T X_\text{o}\, T^{-1} = \Sigma_H^{1/2}$, where Σ_H is called the matrix of Hankel singular values. It is diagonal and contains the eigenvalues of the product $X_\text{c}\, X_\text{o}$ ordered by decreasing magnitude along its diagonal. These values are exactly the ratios $\epsilon_\text{o}/\epsilon_\text{c}$ for each state in the new coordinates. Partitioning the state vector such that x_1 contains the states with large Hankel singular values and x_2 those with small Hankel singular values, system (3) can be written as

$$\begin{aligned} \dot{x}_1 &= A_{11}\, x_1 + A_{12}\, x_2 + B_1\, u \\ \dot{x}_2 &= A_{21}\, x_1 + A_{22}\, x_2 + B_2\, u \\ y &= \ C_1\, x_1 + \ C_2\, x_2 + \ D\, u\ . \end{aligned} \tag{5}$$

The states that are both highly controllable and observable are represented by $z := x_1$. The states x_2 contribute little to the input-output behavior and are removed from the state vector by truncation, leading to a reduced-order model

$$\begin{aligned} \dot{z} &= A_{11}\, z + B_1\, u \\ y &= \ C_1\, z + \ D\, u\ . \end{aligned} \tag{6}$$

For large-scale systems with several thousands of states, the Lyapunov equations (4) become intractable. In this case, low-rank approximations of the Gramians can be used instead. For LTI systems, the controllability Gramian corresponds to $\int_0^\infty e^{A\,t} B\, B^T e^{A^T t} \mathrm{d}t$, or equivalently $\int_0^\infty X(t)\, X^T(t) \mathrm{d}t$, where $X(t) = [e^{A\,t} B_1 \cdots e^{A\,t} B_{n_u}]$ is the state response to Dirac impulses applied individually to all inputs and B_i denotes the ith column of B [5], [15], [16]. These impulse responses can be obtained by simulating the autonomous system $\dot{x} = A\, x$ with initial conditions $x_0 = B_i$ for a sufficiently long time period. A finite number of samples along this state trajectory is collected into a matrix $X_\text{sample} = [X(t_1)\ X(t_2) \ldots X(t_N)]$. An approximation for the infinite integral is then

$$X_\text{c} = \int_0^\infty X(t)\, X^T(t) \mathrm{d}t \approx X_\text{sample}\, X_\text{sample}^T, \tag{7a}$$

so that the rank of the empirical estimate is limited by the number of samples. Completely analogous, an empirical observability Gramian can be obtained as

$$X_\text{o} \approx P_\text{sample}\, P_\text{sample}^T\ , \tag{7b}$$

where $P_\text{sample} = [P(t_1)\ P(t_2) \ldots P(t_N)]$ collects samples of the matrix of state trajectories $P(t) = [e^{A^T t} C_1^T \cdots e^{A^T t} C_{n_u}^T]$, obtained from simulating the adjoint system $\dot{p} = A^T p$. The initial conditions for this simulation are $p_0 = C_i^T$, where C_i denotes the ith row of the matrix C. For further details and generalizations for the approximation of nonlinear systems, see [16]–[18].

While simultaneous observability and controllability is a very useful metric for model order reduction, many engineering problems require the emphasis of a certain frequency region. Balancing and truncation in its standard form solves an approximation problem of the form $\|G(s) - G_\text{approx}(s)\|_\infty < \epsilon$, i. e., there exists an error bound in the $\mathcal{H}_\infty$ norm and thus on the worst error over all frequencies. The frequency-weighted approximation problem, first introduced in [19], is of the form $\|\Omega_\text{o}(s)\,(G(s) - G_\text{approx}(s))\,\Omega_\text{i}(s)\|_\infty < \epsilon$, where $\Omega_\text{o}(s) = C_{\Omega_\text{o}}(sI - A_{\Omega_\text{o}})^{-1} B_{\Omega_\text{o}} + D_{\Omega_\text{o}}$ and $\Omega_\text{i}(s) = C_{\Omega_\text{i}}(sI - A_{\Omega_\text{i}})^{-1} B_{\Omega_\text{i}} + D_{\Omega_\text{i}}$ are stable, minimum phase weighting filters that emphasize a frequency range of interest. Weighted Gramians X_c and X_o

that measure controllability and observability in this frequency range of interest can be calculated by solving the two augmented Lyapunov equations

$$\begin{bmatrix} A & B\,C_{\Omega_\mathrm{i}} \\ 0 & A_{\Omega_\mathrm{i}} \end{bmatrix} \begin{bmatrix} X_\mathrm{c} & \star \\ \star & \star \end{bmatrix} + \begin{bmatrix} X_\mathrm{c} & \star \\ \star & \star \end{bmatrix} \begin{bmatrix} A & B\,C_{\Omega_\mathrm{i}} \\ 0 & A_{\Omega_\mathrm{i}} \end{bmatrix}^T + \begin{bmatrix} B\,D_{\Omega_\mathrm{i}} \\ B_{\Omega_\mathrm{i}} \end{bmatrix} \begin{bmatrix} B\,D_{\Omega_\mathrm{i}} \\ B_{\Omega_\mathrm{i}} \end{bmatrix}^T = 0, \tag{8a}$$

$$\begin{bmatrix} A & 0 \\ B_{\Omega_\mathrm{o}} C & A_{\Omega_\mathrm{o}} \end{bmatrix}^T \begin{bmatrix} X_\mathrm{o} & \star \\ \star & \star \end{bmatrix} + \begin{bmatrix} X_\mathrm{o} & \star \\ \star & \star \end{bmatrix} \begin{bmatrix} A & 0 \\ B_{\Omega_\mathrm{o}} C & A_{\Omega_\mathrm{o}} \end{bmatrix} + \begin{bmatrix} D_{\Omega_\mathrm{o}} C & C_{\Omega_\mathrm{i}} \end{bmatrix}^T \begin{bmatrix} D_{\Omega_\mathrm{o}} C & C_{\Omega_\mathrm{i}} \end{bmatrix} = 0. \tag{8b}$$

The $\star$ in (8) denote block matrices that correspond to filter states and are, in general, of no interest for the model order reduction.

B. Projection Perspective on Model Order Reduction

The truncation that turns (5) into (6) can be expressed as replacing $\left[\begin{smallmatrix} x_1 \\ x_2 \end{smallmatrix}\right]$ with $\left[I_{n_z}\ 0_{n_z \times (n_x - n_z)}\right]^T x_1$ and multiplying the state equation from the left by $\left[I_{n_z}\ 0_{n_z \times (n_x - n_z)}\right]$. An equivalent representation of the balanced reduced-order system (6) is thus

$$\begin{aligned} \dot{z} &= \overbrace{W^T A\, V}^{A_\mathrm{red}} z + \overbrace{W^T B}^{B_\mathrm{red}} u \\ y &= \underbrace{C\, V}_{C_\mathrm{red}} z + D\, u \end{aligned} \tag{9}$$

with $V = T^{-1}\left[I_{n_z}\ 0_{n_z \times (n_x - n_z)}\right]^T$, $W^T = \left[I_{n_z}\ 0_{n_z \times (n_x - n_z)}\right] T$. It is shown in this section that the reduced-order model (9) and hence balancing and truncation is a Petrov-Galerkin approximation of the original system, i. e., an approximation obtained by oblique projection. Taking this perspective allows the extension to LPV systems in Section III-A and to consequently construct an approximation to LPV balancing and truncation in Section III-B.

An oblique projection is a linear operation defined by a matrix $\Pi = V\,(W^T V)^{-1} W^T$ with $V \in \mathbb{R}^{n_x \times n_z}$, $W \in \mathbb{R}^{n_x \times n_z}$ and $\operatorname{rank}(W^T V) = n_z$. Hence, a projection is idempotent, i. e., $\Pi = \Pi^2$. It is completely characterized by its range space $\operatorname{span}(\Pi) = \operatorname{span}(V)$ and its nullspace $\ker(\Pi) = \operatorname{span}\big(\Pi^T\big)^\perp = \operatorname{span}(W)^\perp$. This fact is easy to prove by replacing V and W with their respective thin QR-factorizations. A vector space is said to be projected by Π *along* the orthogonal complement of the subspace spanned by the columns of W and *onto* a subspace spanned by the columns of V. The projection thus restricts the vector space $\mathbb{R}^{n_x}$ to a lower dimensional subspace $\operatorname{span}(V) \subset \mathbb{R}^{n_x}$. Reference [20, Corollary 2.1] shows that any projection can be parameterized by V and a symmetric positive definite matrix $S \in \mathbb{R}^{n_x \times n_x}$ as

$$\Pi = V\ \underbrace{(V^T S\, V)^{-1}\, V^T S}_{W^T}\ . \tag{10}$$

Any W constructed in this way is biorthogonal to V, i. e., $W^T V = I_{n_z}$. Thus, from this point on, biorthogonality of V and W is assumed without loss of generality.

It helps to apply some geometrical interpretation at this point. Given V and W with $W^T V = I_{n_z}$ and a point $x \in \mathbb{R}^{n_x}$, the projection of x lies in the span of V and can hence be written as $V\,z$ with some coefficient vector $z \in \mathbb{R}^{n_z}$. The component of x that is eliminated by the projection is in the nullspace of Π and hence orthogonal to W. This can be stated as $W^T(x - V\,z) = 0$. The projection $\Pi\,x$ can thus be seen as an approximation to x in $\operatorname{span}(V)$ with zero error within $\operatorname{span}(W)$. The subspace $\operatorname{span}(V)$ is consequently termed *basis space* of the approximation and $\operatorname{span}(W)$ is called *test space*.

Model order reduction requires the approximation of a dynamic system given by a differential equation, rather than an approximation for a single point in the state space. The goal is thus to find an approximate solution $x_\mathrm{approx} = V\,z$ to the state equation in (3), i. e.

$$\underbrace{\dot{x}_\mathrm{approx}}_{V\,\dot{z}} \approx A\ \underbrace{x_\mathrm{approx}}_{V\,z} + B\,u\ . \tag{11}$$

From the previous discussion, $V\,z$ is uniquely determined by $z = W^T x$ for given V, W, and x. Hence, the right hand side of (11) is known for a given state x and input u. A solution for the n_z-dimensional vector $\dot{z}$, however, requires the n_x equations imposed by (11) to be satisfied. Consequently, no $\dot{z}$ exists, in general, that exactly satisfies (11). The residual of the approximation is

$$r := V\dot{z} - (A\,V\,z + B\,u)\ . \tag{12}$$

If $\dot{z}$ is now selected such that the residual (12) is restricted to be orthogonal to the test space $\operatorname{span}(W)$, i. e.

$$W^T\,(V\dot{z} - (A\,V\,z + B\,u)) = 0\ , \tag{13}$$

the procedure is known as *Petrov-Galerkin approximation*, see e. g. [16], [21], [22]. The unique solution to (13) is

$$\dot{z} = W^T A\,V\,z + W^T B\,u\ . \tag{14}$$

The desired approximation is hence given by $x_\mathrm{approx} = V\,z$, where z is the solution to (14). Adding the output equation $y = C\,x_\mathrm{approx} + D\,u$ to (14) then yields the reduced-order model (9). This shows, that balancing and truncation is indeed a Petrov-Galerkin approximation.

Given controllability and observability Gramians, obtained by any of the three methods described in Section II-A, this projection can be directly constructed from what is known as the *square root algorithm* [23]. Doing so requires the Cholesky factorizations $X_\mathrm{o} = L_\mathrm{o} L_\mathrm{o}^T$ and $X_\mathrm{c} = L_\mathrm{c} L_\mathrm{c}^T$, as well as the singular value decomposition (SVD) of the product

$$L_\mathrm{c}^T L_\mathrm{o} = \begin{bmatrix} U_1 & U_2 \end{bmatrix} \begin{bmatrix} \Sigma_1 & \\ & \Sigma_2 \end{bmatrix} \begin{bmatrix} N_1 & N_2 \end{bmatrix}^T\ . \tag{15}$$

The singular values are ordered by descending magnitude, such that the diagonal matrix Σ_1 contains the largest n_z singular values. The orthogonal matrices $\left[\begin{smallmatrix} U_1 & U_2 \end{smallmatrix}\right]$ and $\left[\begin{smallmatrix} N_1 & N_2 \end{smallmatrix}\right]$ contain the corresponding left and right singular vectors.[1] The oblique projection for balancing and truncation is

$$\Pi_\mathrm{bal} = \underbrace{L_\mathrm{c}\, U_1\, \Sigma_1^{-1/2}}_{V}\ \underbrace{\Sigma_1^{-1/2} N_1^T\, L_\mathrm{o}^T}_{W^T}\ . \tag{16}$$

[1]The notation N is chosen here to avoid confusion with the matrix V used to denote a basis for the range space of a projection.

The projection is thus onto $\operatorname{span}(L_\mathrm{c}\,U_1)$ and along $\ker\!\left(N_1^T L_\mathrm{o}^T\right)$, where the singular values are a mere scaling of the states, see [16], [23], [24] for details. Another form of this projection will be used throughout Section III. It is formulated in the following proposition.

Proposition 1: Let the controllability and observability Gramians $X_\mathrm{o} = L_\mathrm{o}\,L_\mathrm{o}^T$ and $X_\mathrm{c} = L_\mathrm{c}\,L_\mathrm{c}^T$, and the SVD of the product $L_\mathrm{c}^T L_\mathrm{o} = \begin{bmatrix} U_1 & U_2 \end{bmatrix} \begin{bmatrix} \Sigma_1 & \\ & \Sigma_2 \end{bmatrix} \begin{bmatrix} N_1 & N_2 \end{bmatrix}^T$ be given. Let Q denote a basis for $\operatorname{span}(L_\mathrm{c}\,U_1)$. A projection that achieves balancing and truncation is

$$\Pi_\mathrm{bal} = Q\left(Q^T X_\mathrm{o} Q\right)^{-1} Q^T X_\mathrm{o}\,. \tag{17}$$

Proof: Let $Q\,R$ denote the thin QR-factorization of $L_\mathrm{c}\,U_1$. Replacing Q by $L_\mathrm{c}\,U_1\,R^{-1}$ and X_o by $L_\mathrm{o}\,L_\mathrm{o}^T$ in (17) yields

$$\Pi_\mathrm{bal} = L_\mathrm{c}\,U_1\left(U_1^T L_\mathrm{c}^T L_\mathrm{o}\,L_\mathrm{o}^T L_\mathrm{c}\,U_1\right)^{-1} U_1^T L_\mathrm{c}^T L_\mathrm{o}\,L_\mathrm{o}^T\,.$$

It follows from the given SVD that $U_1^T L_\mathrm{c}^T L_\mathrm{o} = \Sigma_1 N_1^T$. Substitution of this expression results in

$$\Pi_\mathrm{bal} = L_\mathrm{c}\,U_1(\Sigma_1 N_1^T N_1 \Sigma_1)^{-1}\Sigma_1 N_1^T L_\mathrm{o}^T.$$

The equivalence to (16) is established by finally using the fact that $(\Sigma_1 N_1^T N_1 \Sigma_1)^{-1}\Sigma_1 = \Sigma_1^{-1}$. □

III. LPV Model Order Reduction by Parameter-Varying Oblique Projection

Balancing and truncation for an LPV system essentially requires the same steps as in Section II. Once Gramians are computed, a projection for balancing and truncation can be computed in exactly the same way as for LTI systems. Gramians may, however, now themselves depend on the parameter and are no longer unique. They have to be calculated as symmetric positive definite solutions from the optimization

$$\min_{X_{\mathrm{c},\rho}, X_{\mathrm{o},\rho}} \int_{\mathcal{P}} \operatorname{trace}(X_{\mathrm{c},\rho} X_{\mathrm{o},\rho})\,\mathrm{d}\rho \quad \text{s.t.} \quad \forall \rho \in \mathcal{P}$$

$$-\frac{\mathrm{d}}{\mathrm{d}t}X_{\mathrm{c},\rho} + A_\rho\,X_{\mathrm{c},\rho} + X_{\mathrm{c},\rho}A_\rho^T + B_\rho\,B_\rho^T \prec 0\,, \tag{18a}$$

$$\frac{\mathrm{d}}{\mathrm{d}t}X_{\mathrm{o},\rho} + A_\rho^T X_{\mathrm{o},\rho} + X_{\mathrm{o},\rho}\,A_\rho + C_\rho^T C_\rho \prec 0\,. \tag{18b}$$

This generalization was first introduced in [3], [4]. As a consequence, the projection (16) is in general also parameter dependent, i. e. $\Pi_\rho = V_\rho\,W_\rho^T$ with $W_\rho^T V_\rho = I_{n_x}$. Thus, $\dot{x}_\mathrm{approx} = V_\rho\,\dot{z} + \sum_{i=1}^{n_\rho} \frac{\partial V_\rho}{\partial \rho_i}\dot{\rho}_i\,z$ so that the residual for the Petrov-Galerkin approximation becomes

$$r := V_\rho\,\dot{z} + \sum_{i=1}^{n_\rho} \frac{\partial V_\rho}{\partial \rho_i}\dot{\rho}_i\,z - (A_\rho\,V_\rho\,z + B_\rho\,u)\,. \tag{19}$$

The reduced-order LPV model obtained by enforcing the orthogonality constraint $W_\rho^T\,r = 0$ is thus

$$\begin{aligned} \dot{z} &= W_\rho^T\left(A_\rho V_\rho - \sum_{i=1}^{n_\rho} \frac{\partial V_\rho}{\partial \rho_i}\dot{\rho}_i\,z\right) z + W_\rho^T B_\rho\,u \\ y &= C_\rho\,V_\rho\,z + D_\rho\,u\,. \end{aligned} \tag{20}$$

It depends explicitly on the parameter rate $\dot{\rho}$ in addition to the original parameter ρ. This enlarges the parameter space and is not desirable since the complexity of the model is increased. A reduced-order LPV model without the additional rate dependence is obtained only when solutions to (18) are restricted to parameter independent matrices. In this case, more conservative solutions are to be expected. Further, even such parameter independent solutions require extensive computational effort to be calculated by numerical methods.

There are thus two key issues: the introduction of rate dependence as a consequence of parameter-varying projections and the computational limitations associated with determining suitable basis and test spaces for the projection. The purpose of Section III-A is to show that it is possible to overcome the first problem by constructing a parameter-varying projection that does not introduce rate dependence. The second problem is addressed in Section III-B by calculating suitable spaces for approximate balancing of the LPV system from pointwise approximation constraints in the parameter space that are numerically well tractable. The proposed method, summarized in Section III-D, is hence not subject to the computational limitations of the LMI solution.

A. Parameter-Varying Oblique Projections

The reduced-order system (20) from LPV balancing and truncation depends on $\dot{V}_\rho$ but not on the time derivative of W_ρ. Hence, rate dependence in the reduced-order model can be avoided by restricting parameter dependence in the projection to W_ρ and keep V constant. Such a projection is formulated in Proposition 2.

Proposition 2: Let $V \in \mathbb{R}^{n_x \times n_z}$ be a given constant matrix with $\operatorname{rank}(V) = n_z < n_x$ and let $S_\rho\colon \mathbb{R}^{n_\rho} \mapsto \mathbb{R}^{n_x \times n_x}$ be a given symmetric positive definite matrix function. Then,

$$\Pi_\rho = V\,\underbrace{\left(V^T S_\rho\,V\right)^{-1} V^T S_\rho}_{W^T}\,. \tag{21}$$

is a parameter-varying oblique projection and the dynamic LPV system obtained by Petrov-Galerkin approximation with constant basis space $\operatorname{span}(V)$ and parameter-varying test space $\operatorname{span}(W_\rho)$ does not dependent on the rate of parameter variation.

Proof: It is readily verified that $W_\rho^T V = I_{n_z} \forall \rho$ and that hence $\Pi_\rho = \Pi_\rho^2$ is an oblique projection. Further, since V is constant, the projected state space equations (20) simplify to

$$\begin{aligned} \dot{z} &= \overbrace{W_\rho^T A_\rho\,V}^{A_{\mathrm{red},\rho}} z + \overbrace{W_\rho^T\,B_\rho}^{B_{\mathrm{red},\rho}} u \\ y &= \underbrace{C_\rho\,V}_{C_{\mathrm{red},\rho}} z + D_\rho\,u\,. \end{aligned} \tag{22}$$

□

The range of the projection (21) in Proposition 2 is constant but the direction of the projection varies across the parameter space. From the perspective of a Petrov-Galerkin approximation, this means that the orthogonality constraint (13) is enforced over a varying test space $\operatorname{span}(W_\rho)$. Since the basis space $\operatorname{span}(V)$ is constant, state consistency for the reduced-order LPV system is nevertheless preserved with both $x \approx V\,z$ and $\dot{x} \approx V\,\dot{z}$. Thus, system (22) has exactly the structure of the desired reduced-order system (2).

B. Basis and Test Space Construction

Recall from Section II-B and Proposition 1 that balancing and truncation is a Petrov-Galerkin approximation, where the basis and test space are determined from the Gramians. For LPV systems, these Gramians may be parameter varying and their calculation requires the LMI solutions (18), that become intractable for many systems even of moderate state dimension. For a fixed parameter value, the solutions to (18) are given exactly by the solutions to the Lyapunov equations (4). This follows from the fact that $Y - X \prec 0$ for all X and Y that satisfy $A\,X - X\,A^T + B\,B^T \prec 0$, $A\,Y - Y\,A^T + B\,B^T = 0$, see [25, Proposition 4]. Further, interpolation between grid points is smooth for a sufficiently dense grid, since $X_{\mathrm{c},\rho}$ and $X_{\mathrm{o},\rho}$ that satisfy (18) are continuous functions of ρ [3]. A remedy for larger systems is thus to calculate LTI Gramians on a grid of frozen parameters by any of the three methods of Section II, i. e., either by (4), (7) or (8). Interpolation is then used to approximate the parameter-varying Gramians.

Equating the form of a parameter-varying oblique projection in Proposition 2 with the projection for balancing and truncation in Proposition 1, it is clear that the matrix X_{o} is allowed to be parameter dependent. Hence, the parameter-dependent approximation for the observability Gramian can directly be used. Nevertheless, a constant basis $Q \in \mathbb{R}^{n_x \times n_z}$ for the basis space is required to avoid rate dependence in the reduced-order system. In order to reproduce balancing and truncation, Q should be a basis for $\operatorname{span}(L_{\mathrm{c},\rho}\,U_{1,\rho})$, where the span of the parameter-varying matrix refers to the parametrically varying vector space that is spanned by the matrix $L_{\mathrm{c},\rho_k}\,U_{1,\rho_k}$ for fixed values ρ_k. In general, this can only be achieved by a parameter-varying basis Q_ρ, obtained, e. g., from a thin QR factorization at each grid point. The remaining critical question is thus in what sense the constant subspace $\operatorname{span}(Q)$ should approximate the parameter-varying subspace $\operatorname{span}(Q_\rho)$. A practical approach for an optimal approximation over a grid of parameter values $\{\rho_k\}_{k=1}^{n_g}$ is given in the following proposition.

Proposition 3: Let $Q_\rho \in \mathbb{R}^{n_x \times n_z}$ with $Q_\rho^T\,Q_\rho = I_{n_z}$ be a given parameter dependent basis for the parameter-varying subspace $\operatorname{span}(Q_\rho)$. Let further $\begin{bmatrix} Q_{\rho_1} & \cdots & Q_{\rho_g} \end{bmatrix}^T$ denote the collection of function evaluations of Q_ρ on the grid of parameter values $\{\rho_k\}_{k=1}^{n_g}$. Let

$$\begin{bmatrix} \bar{U}_1 & \bar{U}_2 \end{bmatrix} \begin{bmatrix} \bar{\Sigma}_1 & \\ & \bar{\Sigma}_2 \end{bmatrix} \begin{bmatrix} Q & Q_\perp \end{bmatrix}^T = \begin{bmatrix} Q_{\rho_1}^T \\ \vdots \\ Q_{\rho_g}^T \end{bmatrix} \tag{23}$$

be the SVD such that $\bar{\Sigma}_1$ contains the largest n_z singular values and $\bar{\Sigma}_2$ the remaining $n_x - n_z$ singular values. Then, $\operatorname{span}(Q)$ is an optimal approximation for $\operatorname{span}(Q_\rho)$ in the sense that its orthogonal complement $Q_\perp$ minimizes

$$\min_{Q_\perp} \sum_{k=1}^{n_g} \|Q_{\rho_k}^T\,Q_\perp\|_F^2 \quad \text{s.t.} \quad Q_\perp^T Q_\perp = I_{n_x - n_z}\,. \tag{24}$$

Proof: Since the equality $\|X\|_F^2 + \|Y\|_F^2 = \left\|\left[\begin{smallmatrix} X \\ Y \end{smallmatrix}\right]\right\|_F$ holds for all matrices X and Y of compatible dimensions, (24) can be rewritten as

$$\min_{Q_\perp} \left\| \begin{bmatrix} Q_{\rho_1}^T \\ \vdots \\ Q_{\rho_{n_g}}^T \end{bmatrix} Q_\perp \right\|_F^2 \quad \text{s.t.} \quad Q_\perp^T Q_\perp = I_{n_x - n_z}.$$

The minimizer is found from the SVD (23) and the optimal cost is $\|\bar{U}_2\,\bar{\Sigma}_2\|_F^2$. □

Proposition 3 states, that a constant subspace $\operatorname{span}(Q)$ is an optimal approximation for the parameter-varying subspace $\operatorname{span}(Q_\rho)$ if its orthogonal complement $\operatorname{span}(Q_\perp) = \operatorname{span}(Q)^\perp$ approximates the parameter-varying nullspace $\ker\big(Q_\rho^T\big)$. For a single grid point ρ_k, the matrix $Q_{\rho_k}^T\,Q_\perp$ is rank deficient and the optimal "approximation" that attains the exact minimum 0 is simply a basis for the nullspace $\ker\big(Q_{\rho_k}^T\big)$. Obviously, a constant basis cannot, in general, achieve a zero norm for multiple grid points at once if $\operatorname{span}(Q_\rho)$ is not constant. The cost function in (24) thus measures the average "nullspace violation" over all grid points.

This way of choosing a common basis space is, in fact, identical to the approach first proposed in the context of parametric model-order reduction in [13], but Proposition 3 establishes optimality and provides a clear interpretation of the procedure. There remains however a potential hazard with following this purely geometric argument of constructing the basis space: only directionality is considered, regardless of the importance of a direction for input-output behavior. While the n_z most important directions at each grid point are captured within the individual bases Q_{ρ_k}, there is no notion of the relative importance of directions at different grid points. One way of approaching this problem is to weight individual directions in the cost function. With a weighting function $\Lambda_\rho = \operatorname{diag}(\lambda_{1,\rho_k}, \ldots, \lambda_{n_z,\rho_k})$ that consists of scalar weights $\lambda_{i,\rho}$ for the individual basis vectors in Q_{ρ_k}, the objective in (24) becomes

$$\min_{Q_\perp} \sum_{k=1}^{n_g} \left\|\Lambda_\rho\,Q_{\rho_k}^T\,Q_\perp\right\|_F^2 \quad \text{s.t.} \quad Q_\perp^T Q_\perp = I_{n-n_z}\,. \tag{25}$$

A natural choice for Λ_ρ is to take the matrix $\Sigma_{1,\rho}$ from the SVD eq:SVD of the Cholesky factors $L_{\mathrm{c},\rho}^T\,L_{\mathrm{o},\rho}$ and hence to weight the individual directions by their corresponding Hankel singular values.

C. Stability Considerations

If the subspaces are calculated from point-wise solutions, stability guarantees are lost, since the interpolated matrix functions do not necessarily satisfy the LMIs (18) due to the rate term. It is however possible to guarantee stability of the reduced-order model for "slowly" varying parameters when the Gramians are obtained as solutions to the Lyapunov equations (4). A result from [20] and the form of the projection for balancing and truncation given in Proposition 1 are invoked to show that all poles of the reduced-order system are in the left half plane for frozen parameters. Multiplying the Lyapunov equation (4b) for the original system from the left by Q^T and from the right by Q results in

$$Q^T A^T X_{\mathrm{o}}\,Q + Q^T X_{\mathrm{o}}\,A\,Q + Q^T C^T C\,Q = 0\,. \tag{26}$$

Using $A_{\text{red}} = (Q^T X_\text{o} Q)^{-1} Q^T X_\text{o} A Q$ and $C_{\text{red}} = C Q$, it can be shown that (26) is equivalent to

$$A_{\text{red}}^T (Q^T X_\text{o} Q) + (Q^T X_\text{o} Q) A_{\text{red}} + C_{\text{red}}^T C_{\text{red}} = 0. \qquad (27)$$

Since X_o is symmetric positive definite, so is $Q^T X_\text{o} Q$ and consequently A_{red} has all its eigenvalues in the left half plane. This property guarantees stability for sufficiently slow parameter variation, see [26]. When frequency-weighted Gramians or impulse responses are used to construct the projection, even this weaker stability property cannot be guaranteed anymore. It is however worth noting that an a posteriori stability test, that might also include rate bounds, can be performed by solving an LMI feasibility problem of the form $A_{\text{red},\rho}^T X + X_\rho A_{\text{red},\rho} - \sum_{i=1}^{n_\rho} \frac{\partial X_\rho}{\partial \rho_i} \dot{\rho}_i \prec 0$, see [27]. Since this only involves the reduced-order model, the calculation is likely to be tractable, even if it is not for the full order model.

D. Implementation

The proposed model order reduction method is summarized in this section and its implementation is described. For convenience, Matlab notation is used, e. g., $Q(1:n_x, 1:n_z)$ denotes the first $n_x \times n_z$ elements of the matrix Q. A $\star$ again denotes quantities of no interest. The algorithm requires a grid of parameter values $\{\rho_k\}_{k=1}^{n_g}$, and the gridded LPV dynamic system $\{A_{\rho_k}, B_{\rho_k}, C_{\rho_k}, D_{\rho_k}\}_{k=1}^{n_g}$.

The first step is to calculate the Cholesky factors $\{L_{\text{c},\rho_k}\}_{k=1}^{n_g}$ and $\{L_{\text{o},\rho_k}\}_{k=1}^{n_g}$ of the Gramians at each grid point ρ_k by either of the three methods described in Section II. While this is computationally the most challenging part of the reduction, efficient algorithms are readily available. It should be noted that the complete Gramians are never required and that thus Hammarling's algorithm [28] can be used to directly obtain the Cholesky factors from the Lyapunov equations (4) or (8). Similarly, only the matrices of sampled impulse responses in (7) are required, not the full empirical Gramians. Next, the basis space is computed:

for $k = 1$ **to** n_g **do**
  $(U, \Sigma, \star) \leftarrow \text{svd}(L_\text{c}^T L_\text{o})$
  $(\bar{U}, \star, \star) \leftarrow \text{svd}(L_\text{c} U(1{:}n_x, 1{:}n_z))$
  if subspace weighting is desired **then**
    $\Lambda \leftarrow \Sigma(1{:}n_z, 1{:}n_z)$
  else
    $\Lambda \leftarrow I_{n_z}$
  end if
  $\bar{Q}(1{:}n_x, 1{+}n_z\,(k{-}1){:}n_z\,k) \leftarrow \bar{U}(1{:}n_x, 1{:}n_z)\,\Lambda$
end for
$(Q, \star, \star) \leftarrow \text{svd}(\bar{Q})$
$V \leftarrow Q(1{:}n_x, 1{:}n_z)$

The choice of n_z can be guided by the singular values obtained from the first SVD at each grid point, e. g., as $\text{trace}(\Sigma_2^2) < \epsilon$ or as $\text{trace}(\Sigma_1^2)/\text{trace}(\Sigma_2^2) < \epsilon$, where the threshold ϵ reflects a desired accuracy at the grid points. The third step is to calculate a basis for the test space, using a numerically stable implementation of the equation $W_\rho = X_{\text{o},\rho} V (V^T X_{\text{o},\rho} V)^{-1}$:

for $k = 1$ **to** n_g **do**
  $(Q, R) \leftarrow \text{qr}(L_{\text{o},\rho_k}^T V)$
  $W_{\rho_k} \leftarrow L_{\text{o},\rho_k} Q\,(R^T)^{-1}$
end for

In a last step, the state space matrices of the reduced-order system are calculated:

for $k = 1$ **to** n_g **do**
  $A_{\text{red},\rho_k} \leftarrow W_{\rho_k}^T A_{\rho_k} V$
  $B_{\text{red},\rho_k} \leftarrow W_{\rho_k}^T B_{\rho_k}$
  $C_{\text{red},\rho_k} \leftarrow C_{\rho_k} V$
  $D_{\text{red},\rho_k} \leftarrow D_{\rho_k}$
end for

These matrices then represent the gridded reduced-order LPV model and can be interpolated.

IV. Application Examples

This section demonstrates the applicability and effectiveness of the proposed model order reduction method by means of two examples. The first example is a high fidelity longitudinal dynamics model of an aeroservoelastic unmanned aerial vehicle. This multi-input-multi-output system is of moderate size, but poses a challenge due to the strong nonlinear dependence of its dynamic properties on the airspeed. Design of flight control systems for these types of aircraft requires accurate, yet low-order models. The second example is the far wake model of a wind turbine. Such models are relevant to study the aerodynamic interactions in a wind farm and to develop control strategies to maximize the overall power output of several turbines that are located close to each other.

A. Example: Aeroservoelastic Aircraft

A model of the X56 MUTT (Multi Utility Technology Testbed) aircraft is employed to demonstrate the use of the proposed method to obtain a control-oriented low-order model. The X56 is a research platform for control of highly flexible aircraft and currently in use by NASA [29]. A schematic of the aircraft is shown in Fig. 1. A high-fidelity model of the longitudinal dynamics is considered in this paper. It combines rigid-body flight dynamics from first principle modeling, structural dynamics from FEM modeling and unsteady aerodynamics from CFD modeling [30]. The rigid body states are described in the moving body frame and represented in the familiar form as angle of attack α and pitch rate q. The flexible modal displacements are represented in terms of assumed mode shapes and generalized coordinates η. Unsteady aerodynamic

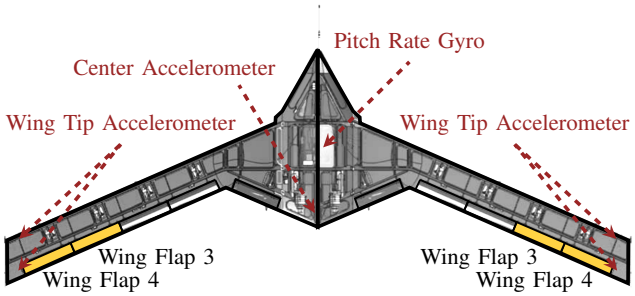

Fig. 1. X56A MUTT unmanned aerial vehicle.

states are represented by w and are related to the rigid and flexible degrees of freedom of the system. Specifically, every degree of freedom is coupled to a third order system that describes the unsteady aerodynamic forces caused by, and acting on, modal displacement. There are 8 structural modes (16 states), the 2 rigid body states and 30 aerodynamic states, which totals to 48 states. As inputs, symmetric deflection of the two outboard wing flap pairs (δ_3 and δ_4), highlighted in Figure 1, are considered. The outputs are a pitch rate measurement q_{meas} and acceleration signal at the center body ($a_{z,\text{center}}$), as well as an averaged wing tip acceleration signal ($a_{z,\text{wing}}$) that combines measurements from the four sensors shown in Fig. 1.

The dynamics of the aircraft depend nonlinearly on the airspeed V_0 and hence the state space model is of the form

$$\begin{aligned} \dot{x} &= A(V_0)\,x + B(V_0)\,\delta \\ y &= C(V_0)\,x + D(V_0)\,\delta\,, \end{aligned} \tag{28}$$

with state vector $x = \left[w^T \mid \alpha \quad q \mid \dot{\eta}^T \mid \eta^T\right]^T$, output vector $y = [q_{\text{meas}}\ a_{z,\text{center}}\ a_{z,\text{wing}}]^T$, and input vector $\delta = [\delta_3\ \delta_4]^T$. A grid representation with 12 uniformly spaced points is used to cover the domain $V_0 \in [30.6 \quad 68]$m/s. The aircraft is naturally stable in this domain but the damping ratio of the lowest-frequency aeroelastic mode decreases dramatically with higher airspeeds. Hence, the dynamics change rapidly.

For a control-oriented model, the available bandwidth of a control system provides an upper frequency limit on the fidelity requirement. Frequency weighting is thus especially useful for this type of model. Fifth order butterworth filters with a cut-off frequency of 100 rad/s are selected for the present example. The augmented Lyapunov equations (8) are solved using the Matlab routine `lyapchol` at each grid point. The basis space is determined by weighting each direction with its corresponding singular value as described in Section III-B. The calculation takes only seconds and hence the order of the reduced model can be determined by trial and error. A 12th order model yields satisfactory results.

Figure 2 shows the Bode magnitude plots of the full-order and the reduced-order model evaluated for frozen parameter values at the grid points. The reduced-order model agrees very well with the full-order model up the specified frequency of 100 rad/s. Larger discrepancies are only noticeable for the center acceleration output from 20 rad/s onwards but only appear where the magnitude is low. Figure 3 shows the step response of both the full-order and the reduced-order model along a time-varying parameter trajectory. The trajectory covers the complete parameter space with a high rate of variation. The reduced-order model nevertheless approximates the response very well, also for the center acceleration signal. The most prominent difference is visible in the high frequency transients right after that step input is applied. The reduced-order model clearly omits these as a consequence of the frequency weighted approximation. Figure. 4 shows the pole migration of both models over the parameter space with linear interpolation in between grid points. The plot confirms that the reduced-order model obtained by parameter-varying projection indeed retains continuous dependence on the parameter. It further shows that the loci of the lightly damped modes in reduced-order model almost exactly coincide with those of the original system. This is important, e. g., in order to perform flutter analyses on the reduced-order model.

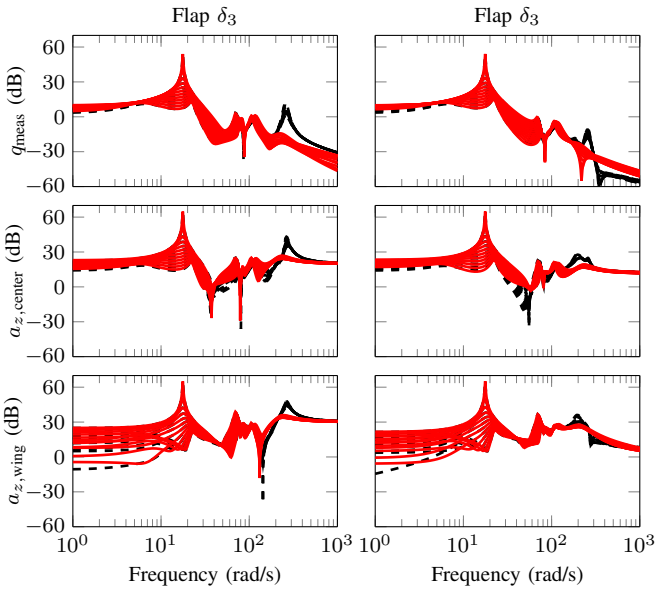

Fig. 2. Frequency responses for frozen parameter values: full-order model (- - - 48 states) and reduced-order (—— 12 states).

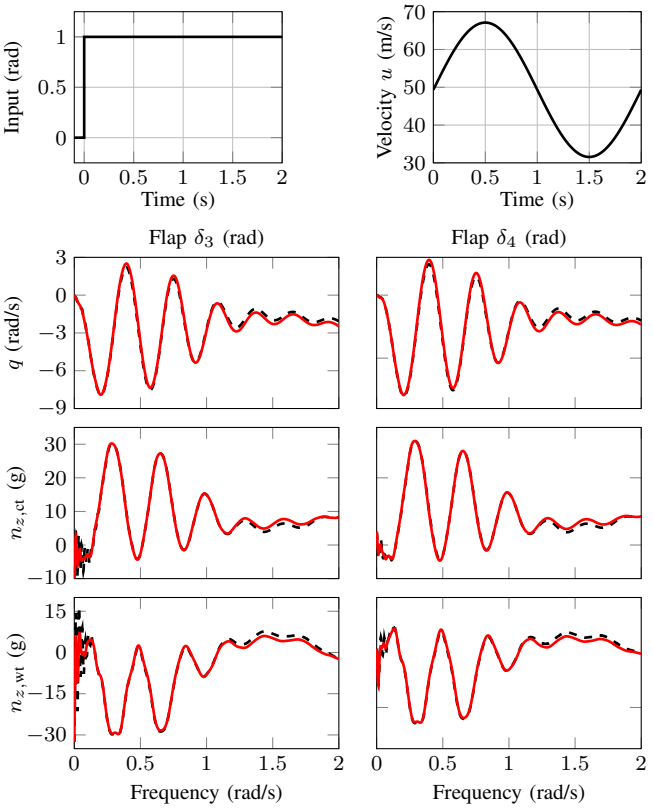

Fig. 3. LPV Simulation of a step response with varying parameter: full-order model (- - - 48 states) and reduced-order (—— 12 states).

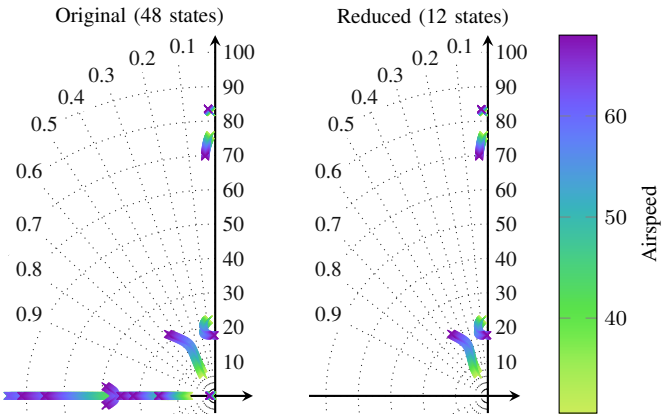

Fig. 4. Pole migration across flight envelope for full and reduced-order model.

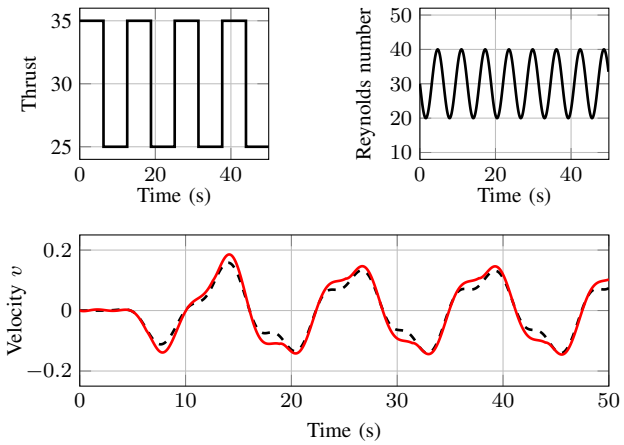

Fig. 5. Nonlinear simulation with fast varying parameter: full-order model (- - - 20502 states) and reduced-order (—— 6 states).

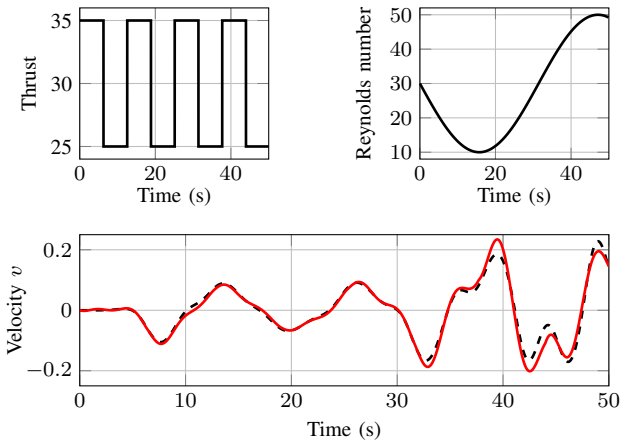

Fig. 6. Nonlinear simulation of with slow varying parameter: full-order model (- - - 20502 states) and reduced-order (—— 6 states).

B. Large-Scale Example: Far Wakes in a Wind Farm

As a second example, an unsteady aerodynamics problem known as the *actuator disk model* [31]–[33] is considered. It can be used to accurately model the far wake of a wind turbine by solving the two-dimensional Navier-Stokes equations for incompressible flows. The streamwise (x) and spanwise (y) velocity components are denoted u and v and their dynamics are governed by the partial differential equations

$$\frac{\partial u}{\partial x}+\frac{\partial v}{\partial y}=0 \tag{29a}$$

$$\frac{\partial u}{\partial t}+u\frac{\partial u}{\partial x}+v\frac{\partial u}{\partial y}=-\frac{1}{\rho}\frac{\partial P}{\partial x}+\nu\left(\frac{\partial^2 u}{\partial x^2}+\frac{\partial^2 u}{\partial y^2}\right)+f \tag{29b}$$

$$\frac{\partial v}{\partial t}+u\frac{\partial v}{\partial x}+v\frac{\partial v}{\partial y}=-\frac{1}{\rho}\frac{\partial P}{\partial y}+\nu\left(\frac{\partial^2 v}{\partial x^2}+\frac{\partial^2 v}{\partial y^2}\right) \tag{29c}$$

where ν is the kinematic viscosity and P is the pressure distribution. The forcing term f depends linearly on the thrust coefficient C_T of the turbine. This coefficient can be changed on a wind turbine via blade pitch or a change of the tip speed ratio and is thus a control input.

The particular configuration studied in this paper consists of two wind turbines, each with rotor diameter d, that are located $5\,d$ apart from each other in a two-dimensional stream of air. A prescribed inflow and a convective outflow condition are used, leading to the boundary conditions

$$\begin{aligned} u_{|x=0}&=U_\infty, & \frac{\partial u}{\partial t}_{|x=20\,d}+U_\infty\frac{\partial u}{\partial x}_{|x=20\,d}&=0,\\ v_{|x=0}&=0, & \frac{\partial v}{\partial t}_{|x=20\,d}+U_\infty\frac{\partial v}{\partial x}_{|x=20\,d}&=0. \end{aligned} \tag{29d}$$

The upstream turbine runs with a constant thrust coefficient, while the downstream turbine's thrust coefficient is considered as a control input. The output is a measurement of the spanwise velocity component v, located $5\,d$ downstream from the second turbine, indicating far wakes. The partial differential equations are solved following standard computational fluid dynamics methods with a central difference scheme for spatial discretization. The grid is defined by 201 points in the streamwise direction and 51 points in the spanwise direction. The discretization yields an ordinary differential equation system with 20502 states that dependents parametrically on the freestream velocity U_∞, or in nondimensionalized form on the Reynolds number Re.

Solving Lyapunov equations for a linearization of this large-scale system is intractable and hence empirical Gramians are constructed from simulation data as described in Section II-A. The matrices of sampled impulse responses are calculated for constant parameter values on the grid $Re = \{10, 20, 30, 40, 50\}$. A forward Euler scheme and time steps of $t_s = 0.01$ s are used for time propagation with a time horizon of $t_N = 50$ s. The resulting trajectories are sampled every 0.5 s and consequently the empirical Cholesky factors at each grid point are of size 20502×100. These Cholesky factors are used exactly as described in Section III-B to construct a parameter-varying oblique projection, without either additional frequency or subspace weights. Simulation results for a sequence of step inputs and two different parameter trajectories are shown in Fig. 5 and Fig. 6. The responses of the reduced-order model are in excellent agreement with the full-order model. The speed of parameter variation appears to have no impact on the quality of the approximation, confirming that there is no neglected rate-dependence in the reduction.

While the quality of the reduction should be strictly judged

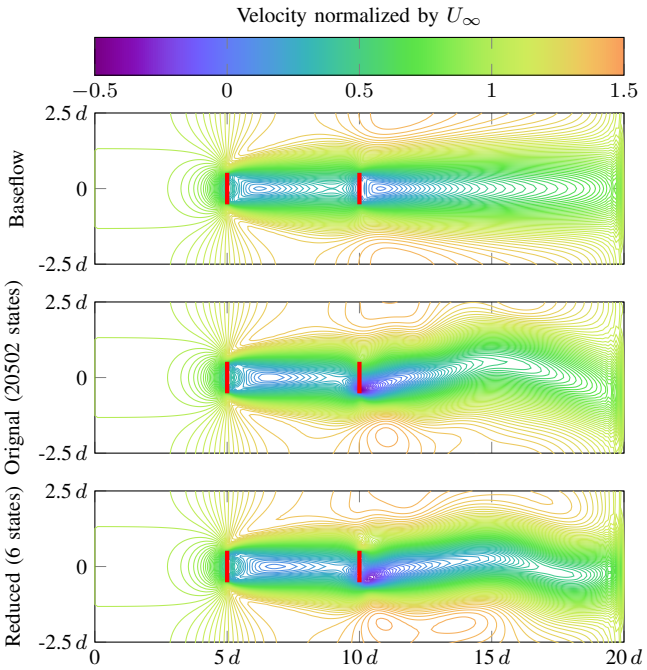

Fig. 7. Streamwise velocities u at $t = 40\,\mathrm{s}$ corresponding to the simulation shown in Fig. 6 with locations of turbines (|).

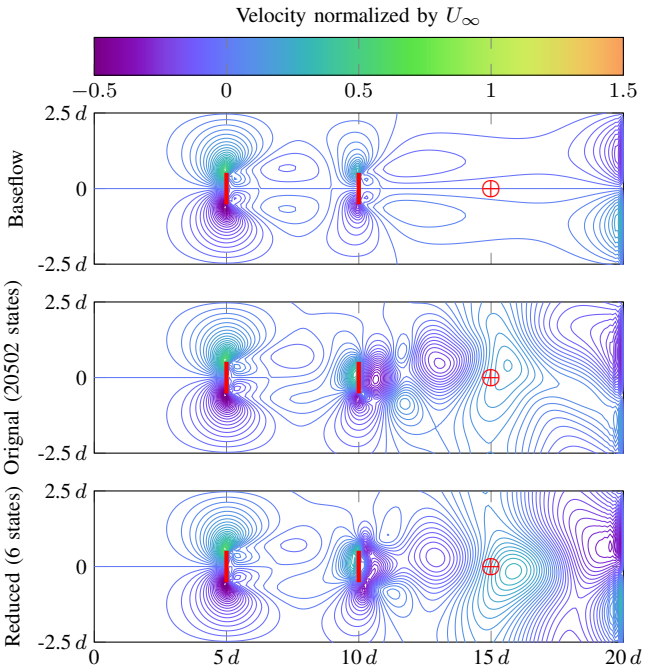

Fig. 8. Spanwise velocities v at $t = 40\,\mathrm{s}$ corresponding to the simulation shown in Fig. 6 with locations of turbines (|) and velocity measurement (⊕).

by how well the reduced-order system captures the considered input-output behavior, it remains insightful to also take a look at the approximated state vector $x_{\text{approx}} = V z$. For the considered problem, the state vector has a clear physical interpretation, namely velocities in x and y direction at each of the 10251 nodes in the domain. Figures 7 and 8 depict the baseflow that corresponds to a constant thrust coefficient $C_T = 30$ for both turbines and frozen-in-time snapshots taken from the simulation shown in Fig. 6. As expected, the reduced-order model is not able to completely resolve the full state accurately. Still, characteristic features of the stream are preserved up to the the measurement point. The states of the reduced-order model can thus still be related to physically meaningful quantities. Velocities further downstream have little importance for the considered output and are hence less accurately resembled by the reduced-order model.

V. Conclusion and Extensions

A. Conclusion

A model order reduction method for LPV systems is developed in this paper. The key technical contribution is the use of a parameter-varying projection that maintains a well-defined LPV system with consistent states across the parameter domain. This projection uses a partially parameter dependent transformation, but in contrast to general parameter-varying state space transformations does not introduce additional rate dependence. It thus provides a middle ground between the potentially conservative use of constant transformations and the increase in complexity that comes with parameter dependent transformations. It is shown that the projection has an immediate application to approximate balanced truncation and related approaches that employ Gramians to quantify the importance of subspaces for model order reduction.

Two detailed application examples are given in this paper. The first example demonstrates the application of the method to a high-fidelity model of an aeroservoelastic unmanned aerial vehicle. The second example is concerned with reducing the model of the unsteady aerodynamics in a wind farm, described by the two-dimensional Navier-Stokes equations for incompressible flows.

B. Extensions

The proposed extension of the general projection framework to parameter-varying projections does not rely on a particular choice of basis and test spaces. Suitable subspaces for the projection can thus not only be calculated by the Gramian-based approach pursued in this paper, but also by entirely different means. For instance, moment matching with Krylov subspaces could be applied. Another possible extension is that to unstable systems. Many systems, particularly in the field of aeroelastic systems, become unstable for some parameter values. The aircraft considered in Section IV-A, e. g., becomes unstable for larger airspeeds. Model-order reduction for unstable LPV systems remains a challenging open topic and adapting the method developed in this paper is ongoing work that also involves finding suitable alternatives for the quantification of the importance of a subspace.

Acknowledgment

The authors thank Brian Danowsky, Chase Schulze, and Thuan Lieu for providing the X-56 model, as well as Jen Annoni for providing the wind farm model.

REFERENCES

[1] F. Wu, X. Yang, A. Packard, and G. Becker, "Induced $\mathcal{L}_2$-norm control for LPV systems with bounded parameter variation rates," *International Journal of Robust and Nonlinear Control*, vol. 6, pp. 2379–2383, 1996.

[2] A. Hjartarson, A. Packard, and P. Seiler, "LPVTools: A toolbox for modeling, analysis, and synthesis of parameter varying control systems," in *1st IFAC Workshop Linear Parameter Varying Syst.*, 2015.

[3] G. D. Wood, "Control of parameter-dependent mechanical systems," Ph.D. dissertation, Univ. Cambridge, 1995.

[4] G. D. Wood, P. J. Goddard, and K. Glover, "Approximation of linear parameter-varying systems," in *IEEE Conference on Decision and Control*, vol. 1, 1996, pp. 406–411.

[5] B. C. Moore, "Principal component analysis in linear systems: Controllability, observability, and model reduction," *IEEE Transactions on Automatic Control*, vol. 26, no. 1, pp. 17–32, 1981.

[6] D. Amsallem and C. Farhat, "An online method for interpolating linear parametric reduced-order models," *SIAM Journal on Scientific Computing*, vol. 33, no. 5, pp. 2169–2198, 2011.

[7] C. Poussot-Vassal and C. Roos, "Generation of a reduced-order LPV/LFT model from a set of large-scale MIMO LTI flexible aircraft models," *Control Engineering Practice*, vol. 20, pp. 919–930, 2012.

[8] F. Adegas, I. Sonderby, M. Hansen, and J. Stoustrup, "Reduced-order LPV model of flexible wind turbines from high fidelity aeroelastic codes," in *IEEE Conference on Control Applications*, 2013, pp. 424–429.

[9] J. Theis, B. Takarics, H. Pfifer, G. Balas, and H. Werner, "Modal matching for LPV model reduction of aeroservoelastic vehicles," in *AIAA Science and Technology Forum and Exhibition*, 2015.

[10] Y. Wang, H. Song, K. Pant, M. J. Brenner, and P. Suh, "Model order reduction of aeroservoelastic model of flexible aircraft," in *AIAA Science and Technology Forum and Exhibition*, 2016, p. 1222.

[11] P. Benner, S. Gugercin, and K. Willcox, "A survey of model reduction methods for parametric systems," Max Planck Institute, Magdeburg, Germany, Tech. Rep. MPIMD/13-14, Aug. 2013. [Online]. Available: http://www2.mpi-magdeburg.mpg.de/preprints/2013/14/

[12] U. Baur, C. Beattie, P. Benner, and S. Gugercin, "Interpolatory projection methods for parameterized model reduction," *SIAM Journal on Scientific Computing*, vol. 33, no. 5, pp. 2489–2518, 2011.

[13] H. Panzer, J. Mohring, R. Eid, and B. Lohmann, "Parametric model order reduction by matrix interpolation," *Automatisierungstechnik*, vol. 8, pp. 475–484, 2010.

[14] J. Theis, P. Seiler, and H. Werner, "Model order reduction by parameter-varying oblique projection," in *to appear in American Control Conference*, 2016, preprint available online at www.aem.umn.edu/%7EAeroServoElastic/Papers/2016/TheisEtAl_16ACC_ModelOrderReductionByParameterVaryingObliqueProjection.pdf.

[15] T. Kailath, *Linear Systems*. Englewood Cliffs, NJ: Prentice Hall, 1980.

[16] A. Antoulas, *Approximation of Large-Scale Dynamical Systems*. Philadelphia, PA: SIAM, 2005.

[17] K. Willcox and J. Peraire, "Balanced model reduction via the proper orthogonal decomposition," *AIAA Journal*, vol. 40, no. 11, pp. 2323–2330, 2002.

[18] S. Lall, J. E. Marsden, and S. Glavaški, "A subspace approach to balanced truncation for model reduction of nonlinear control systems," *International Journal of Robust and Nonlinear Control*, vol. 12, no. 6, pp. 519–535, 2002.

[19] D. Enns, "Model reduction with balanced realizations: An error bound and a frequency weighted generalization," in *Conference on Decision and Control*, 1984.

[20] C. de Villemagne and R. Skelton, "Model reductions using a projection formulation," *International Journal of Control*, vol. 46, no. 6, pp. 2141–2169, 1987.

[21] Y. Saad, *Iterative methods for sparse linear systems*. SIAM, 2000.

[22] M. Rathinam and L. Petzold, "A new look at proper orthogonal decomposition," *SIAM Journal on Numerical Analysis*, vol. 41, no. 5, pp. 1893–1925, 2003.

[23] A. J. Laub, M. T. Heath, C. C. Paige, and R. C. Ward, "Computation of system balancing transformations and other applications of simultaneous diagonalization algorithms," *IEEE Transactions on Automatic Control*, vol. 32, no. 2, pp. 115–122, 1987.

[24] A. Varga, "Balancing free square-root algorithm for computing singular perturbation approximations," in *IEEE Conference on Decision and Control*. IEEE, 1991, pp. 1062–1065.

[25] G. E. Dullerud and F. Paganini, *A course in robust control theory: a convex approach*, ser. Texts in Applied Mathematics. New York: Springer Science & Business Media, 2000, vol. 36.

[26] C. Desoer, "Slowly varying system x= A(t) x," *IEEE Transactions on Automatic Control*, vol. 14, no. 6, pp. 780–781, 1969.

[27] F. Wu, "Control of linear parameter varying systems," Ph.D. dissertation, Univ. California, Berkeley, 1995.

[28] S. Hammarling, "Numerical solution of the stable, non-negative definite lyapunov equation lyapunov equation," *IMA Journal of Numerical Analysis*, vol. 2, no. 3, pp. 303–323, 1982.

[29] J. J. Ryan, J. T. Bosworth, J. J. Burken, and P. M. Suh, "Current and future research in active control of lightweight, flexible structures using the x-56 aircraft," in *AIAA Science and Technology Forum and Exhibition*, 2014.

[30] P. C. Schulze, B. Danowsky, and T. Lieu, "High fidelity aeroservoelastic model reduction methods," in *AIAA Science and Technology Forum and Exhibition*, no. 2016-2007, 2016.

[31] J. N. Sørensen and A. Myken, "Unsteady actuator disc model for horizontal axis wind turbines," *Journal of Wind Engineering and Industrial Aerodynamics*, vol. 39, no. 1, pp. 139–149, 1992.

[32] J. N. Sørensen and C. W. Kock, "A model for unsteady rotor aerodynamics," *Journal of Wind Engineering and Industrial Aerodynamics*, vol. 58, no. 3, pp. 259–275, 1995.

[33] J. Annoni, J. Nichols, and P. Seiler, "Wind farm modeling and control using dynamic mode decomposition," in *AIAA Science and Technology Forum and Exhibition*, no. 2016-2201, 2016.

PLACE PHOTO HERE

Julian Theis Biography text here.

PLACE PHOTO HERE

Peter Seiler Biography text here.

PLACE PHOTO HERE

Herbert Werner Biography text here.